Dynamical properties of low dimensional $CuGeO_3$ and NaV_2O_5 spin-Peierls systems

David Augier and Didier Poilblanc
Laboratoire de Physique Quantique & Unité Mixte de Recherche CNRS 5626
Université Paul Sabatier, 31062 Toulouse, France.
(July 97)

Properties of low-dimensional spin-Peierls systems are described by using a one dimensional $S = \frac{1}{2}$ antiferromagnetic Heisenberg chain linearly coupled to a single phonon mode of wave vector π (whose contribution is expected to be dominant). By exact diagonalizations of small rings with up to 24 sites supplemented by a finite size scaling analysis, static and dynamical properties are investigated. Numerical evidences are given for a spontaneous discrete symmetry breaking towards a spin gapped phase with a frozen lattice dimerization. Special emphasis is put on the comparative study of the two inorganic spin-Peierls compounds $CuGeO_3$ and NaV_2O_5 and the model parameters are determined from a fit of the experimental spin gaps. We predict that the spin-phonon coupling is 2 or 3 times larger in NaV_2O_5 than in $CuGeO_3$. Inelastic neutron scattering spectra are calculated and similar results are found in the single phonon mode approximation and in the model including a static dimerization. In particular, the magnon $S = 1$ branch is clearly separated from the continuum of triplet excitations by a finite gap.

PACS numbers: 64.70.Kb, 71.27.+a, 75.10.Jm, 75.40.Mg, 75.50.Ee

I. INTRODUCTION

Recently, a renewed interest for one dimensional (1D) spin chains was created by the observation of spin-Peierls transitions in the inorganic compounds $CuGeO_3$ [1] and α'-NaV_2O_5 [2–5]. Below some critical temperature T_{SP}, the spin-Peierls phase is experimentally inferred from a rapid drop of the spin susceptibility. The low temperature phase is characterized by the opening of a spin gap Δ (see below) and the dimerization of the lattice along the chain direction as confirmed for example by X-rays diffraction in $CuGeO_3$ [6] and NaV_2O_5 [3] or by Na NMR experiments in NaV_2O_5 [4].

In general, these compounds are well described above the transition temperature by a 1D frustrated antiferromagnetic (AF) Heisenberg chain. The nearest neighbor and next-nearest neighbor spin exchange integrals J and J' can be determined by a fit of the magnetic susceptibility χ at high temperatures. In fact the position of the maximum of the curve and more generally the magnetic properties only depend on the frustration ratio $\alpha = J'/J$.

Parameters such as $J = 160\ K$ and $\alpha = 0.36$ [7] or $J = 150\ K$ and $\alpha = 0.24$ [8] have been suggested for $CuGeO_3$. Further studies [9,10] seem to confirm that the dimerization is large in this system and we shall take $\alpha = 0.36$ in the rest of the paper. For the novel NaV_2O_5 system $J = 440\ K$ and $\alpha \approx 0$ have been proposed [5] in good agreement with Refs. [2,11].

The zero temperature spin gap Δ has been determined by several means. Inelastic neutron scattering (INS) gives a direct measure of it. So far INS has been performed on single crystals of $CuGeO_3$ and powder NaV_2O_5 samples. Values of $\Delta \simeq 2.1$ meV [12,13] and $\Delta = 9.8$ meV [3] have been reported, respectively. Other more indirect methods like NMR can also provide a measure of the magnitude of the spin gap. ^{63}Cu or ^{65}Cu NMR have been performed on single crystals of $CuGeO_3$ [14] and ^{23}Na NMR on aligned polycrystals of NaV_2O_5 [4]. The local magnetic susceptibility is proportional to the NMR Knight shift and the spin gap is estimated by a fit of the temperature dependence of the local susceptibility below the transition temperature. A value of $\Delta \simeq 8.4$ meV was found for NaV_2O_5. A third independent estimation of Δ can be obtained by a fit of the low temperature bulk magnetic susceptibility of single crystals measured for instance by a SQUID-magnetometer technique. Ref. [5] reports a value of $\Delta \simeq 7.3$ meV for NaV_2O_5.

The dimensionless ratio Δ/J is the crucial parameter needed in our theoretical analysis. Results for $CuGeO_3$ are now well established and the value of $\Delta/J = 0.151$ is often used in the literature. Nonetheless ratios such as $\Delta/J = 0.203$ [3], $\Delta/J = 0.175$ [4] or $\Delta/J = 0.193$ [5] can be found for NaV_2O_5. Since this last estimation was obtained from experiments performed on single crystals we have thus decided to use it as a reference. In any case, the quite small differences between the previous experimental values are not relevant.

Theoretically, the spin dynamics of the 1D Heisenberg chain depends strongly on the frustration parameter α. Indeed, for $\alpha > \alpha_c \simeq 0.241$ a gap appears in the spin excitation spectrum [15,16]. Therefore, we expect that the two previous spin-Peierls compounds will have quite different magnetic properties. $CuGeO_3$ is dominated by intrachain frustration. On the other hand, NaV_2O_5 will behave, at high temperatures, more closely to an unfrus-

trated Heisenberg chain and, at low temperatures, the small interchain frustration alone cannot be responsible for the opening of a spin gap. The coupling to the lattice is therefore expected to play a dominant role in the transition at least for NaV_2O_5. In order to study their interplay, the frustration and the spin-lattice coupling have to be treated on equal footings. This is the purpose of this paper.

It is well known that a $1D$ system shows no phase transition at finite temperature because of quantum fluctuations. Interchain couplings are necessary to obtain a finite transition temperature. However, they are thought to be small and will be neglected hereafter in the study of zero temperature properties.

So far, there have been various attempts to treat the coupling to the lattice by considering a static dimerization δ of the exchange integral (so called adiabatic approximation or frozen phonon approximation). The value of δ is determined in order to obtain the experimental value of the zero temperature spin gap Δ. Dimerizations such as $\delta = 0.014$ [7] and $\delta = 0.048$ [17] were proposed for $CuGeO_3$ and for NaV_2O_5, respectively, in order to reproduce the measured spin gaps (assuming $\Delta \simeq 0.151J$ and $\Delta \simeq 0.193J$ for $CuGeO_3$ and NaV_2O_5, respectively). Calculations using this approach have been performed in order to make first comparisons with experiments [9,18–20].

In this paper we use a modification of the previous static model to describe the physical properties of one-dimensional spin-Peierls compounds below the transition temperature. For convenience, the previous *ad hoc* static dimerization discussed above is replaced here by a single dynamical optical phonon mode (Section II). As far as thermodynamic properties are concerned, this model should be, in fact, equivalent *in the thermodynamic limit* to a model where the lattice is treated at a mean field level [21]. However, this new approach has some advantages: (i) it incorporates automatically the elastic energy and avoids the lengthy iterative procedure needed in a mean-field treatment to converge to the equilibrium static lattice dimerization; (ii) it enables to study the mechanism of the lattice symmetry breaking and, hence, provides a basis for future studies including a macroscopic number of phonon modes (i.e. proportional to the system length L) [22] in spin-Peierls chains.

Within this single mode approximation, we truncate the Hilbert space of the phonons and show in details that this approximation is well controlled (Section III). Using a finite size scaling analysis (discussed in detail in Section IV) the dimerization and the spin gap resulting from a spontaneous discrete symmetry breaking of the lattice periodicity are calculated (Section V). Focussing primarily on $CuGeO_3$ and NaV_2O_5 materials, we then establish a simple relation between the parameters of the model in such a way to enforce the constraint that the numerically calculated spin gap is equal to the experimental gap. The role of the parameters is discussed. In the last part (Section VI), we study the spin dynamics. In particular, we investigate the role of the lattice dynamics on the low energy magnon branch and low energy structures in the dynamical spin structure factor. Our results are compared to the ones obtained in the static model [17,19,23,24].

II. MODELS

Our starting point is the 1D frustrated AF Heisenberg chain. For practical applications, the previous values of J and α will be used : $J = 160\ K$, $\alpha = 0.36$ for $CuGeO_3$ [7] and $J = 440\ K$, $\alpha = 0$ for NaV_2O_5 [5]. In addition, a coupling between spins and dispersionless optical phonons (magneto-elastic coupling) is considered. For sake of simplicity we assume a linear dependence of the exchange integrals on the relative atomic displacements $\{u_i\}$ [25,26],

$$H = J\sum_i((1+\lambda u_i)\ \vec{S}_i.\vec{S}_{i+1} + \alpha\vec{S}_i.\vec{S}_{i+2}) + H^0_{\rm ph}, \quad (1)$$

where λ is the coupling constant. $H^0_{\rm ph}$ is the phononic Hamiltonian of identical independent quantum oscillators, $H^0_{\rm ph} = \sum_i(\frac{p_i^2}{2m} + \frac{1}{2}K\,u_i^2)$ (p_i is the conjugate momentum associated to the atomic displacement u_i). The atomic displacements u_i and their conjugate variables can easily be expressed in term of the canonical phonon creation and annihilation operators $b_k^\dagger$ and b_k. Since the spin susceptibility diverges (for $\alpha < 0.5$ [27,28]) at momentum $k = \pi$ we expect that the coupling to the lattice will be dominant at $k = \pi$ which corresponds, in fact, to the modulation of the spin-Peierls ground state. Therefore, from now on, we shall only keep a single $k = \pi$ phonon mode [29]. In this case, using,

$$u_i \simeq (-1)^i\sqrt{\frac{1}{2mL\Omega}}(b_\pi + b_\pi^\dagger)$$

($\Omega^2 = K/m$ and L is the number of sites), the final Hamiltonian becomes,

$$H{=}J\sum_i\left\{\left(1+\tfrac{g\,(-1)^i}{\sqrt{L}}(\ b_\pi + b_\pi^\dagger)\right)\ \vec{S}_i.\vec{S}_{i+1} + \alpha\vec{S}_i.\vec{S}_{i+2}\right\} + H^0_{\rm ph}, \quad (2)$$

where $g = \lambda\sqrt{\frac{1}{2m\Omega}}$ is the dimensionless coupling constant. Within this approximation $H^0_{\rm ph}$ can be rewritten as $H^0_{\rm ph} = \Omega\ (b_\pi^\dagger b_\pi + \frac{1}{2})$ where Ω is the energy of a phononic quantum.

Before going further, we can already discuss qualitatively the physics contained in Hamiltonian (2). Indeed, we expect in the thermodynamic limit a discrete symmetry breaking corresponding to a doubling of the unit-cell. This can be described very simply at the MF level. By assuming a dimerization δ given by the order parameter

$\frac{g}{\sqrt{L}}\langle b_\pi + b_\pi^\dagger\rangle_{MF}$ and omitting a constant part, the MF Hamiltonian takes the form,

$$H_{\rm MF} = J\sum_i((1+\delta(-1)^i)\vec{S}_i.\vec{S}_{i+1} + \alpha\vec{S}_i.\vec{S}_{i+2}) + \tfrac{1}{2}L\tfrac{K}{\lambda^2}\delta^2, \quad (3)$$

where the last term is the elastic energy loss. This is exactly the well known model describing a static dimerization below the transition temperature in spin-Peierls systems [7,8]. Interestingly enough, a similar effective model has also been used to describe conjugated hydrocarbons with bond alternation such as polyacetylene [30]. In this new form, the breaking of the lattice periodicity is explicit. As a consequence the ground state becomes doubly degenerate (the order parameter δ can take a positive or a negative value) and a spin gap appears. The spin-Peierls ground state is characterized by a "$\cdots A-B-A-B\cdots$" pattern with a succession of strong singlet A bonds and weak singlet B bonds (so called Valence Bond or dimer state). Note that δ in model (3) is a variational parameter to be determined in order to minimize the ground state energy by an iterative procedure. In contrast, the dimerization in Hamiltonian (2) arises from a dynamical symmetry breaking. However, it is interesting to notice that models (3) and (2) should be in fact equivalent [31] in the *thermodynamic limit*, at least as far as their thermodynamic properties are concerned [21,32].

Static and dynamical quantities are given by exact diagonalizations of small chains. Using a finite size scaling analysis, results in the thermodynamic limit are deduced. The parameters δ on one hand and g and Ω/J on the other hand are determined from a fit to the experimental spin gap.

III. TRUNCATION PROCEDURE

Let us now deal first with the numerical treatment of (2). The total Hilbert space can be written as the tensorial product of the space of the spin configurations (to which the symmetry group of the problem is applied) times the phononic space. However, strictly speaking, the Hilbert space associated to the phonons is infinite even for a chain of finite length. Indeed, the natural basis $\{|n\rangle\}$ is simply defined by the unlimited occupation number n of the $k=\pi$ phonon mode, $|n\rangle = 1/\sqrt{n!}\,(b_\pi^\dagger)^n|0\rangle$. Such a difficulty can nevertheless be easily handled in an exact diagonalization treatment [33]. The solution is to truncate the phononic space so that the occupation number is smaller than a fixed $N_{\rm max}$ which has to be chosen in an appropriate way. Clearly, if $N_{\rm max}$ is, let us say, an order of magnitude larger than the exact mean occupation number $\langle b_\pi^\dagger b_\pi\rangle$ the truncation procedure will not affect the accuracy of the results which can then be considered as basically exact. This can be seen in Fig. 1 showing the energy per site of the ground state in the spin 0 and 1 sectors (the value of α corresponds to the case of $CuGeO_3$ and a coupling constant $g=0.5$ is used) for chains of length $L=12$ and 20 plotted as a function of $N_{\rm max}$. Typically, the mean occupation number is smaller than 3 as in Figs. 2 and 3 (and in fact even smaller than ~ 0.5 for more realistic parameters) and the energy has converged for $N_{\rm max}\sim 30$. Fig. 1 proves that the truncation procedure is very well controlled even for rather (unphysically) large coupling constants like $g=0.5$. The results reported in the rest of this paper are then obtained with a sufficiently large value of $N_{\rm max}$ and the preliminary studies of the convergence of the results with increasing $N_{\rm max}$, although not mentioned each time, have been performed for each choice of the parameters of the model.

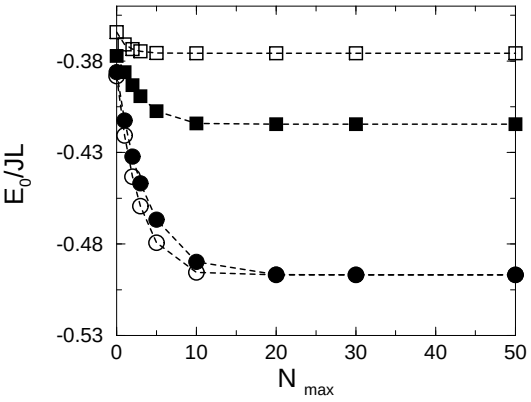

FIG. 1. Convergence of the energy per site of the lowest singlet ($\circ, \bullet$) and triplet ($\Box, \blacksquare$) states in units of J as a function of the maximum number of phonons $N_{\rm max}$. Parameters are $\alpha=0.36$, $g=0.5$ and $\Omega=0.3J$. Open (filled) symbols correspond to $L=12$ ($L=20$) sites.

It is interesting to study the dependence of the mean occupation number on the three parameters of the problem (length of the chain L, coupling constant g and frequency of the phonons Ω) since, first, this number directly determines the practical value of $N_{\rm max}$ to be chosen and, secondly, it provides some physical understanding. Fig. 1 already suggests that the mean occupation number increases with the length of the chains. To investigate this effect in more details, the mean occupation number $\langle\Psi_0|b_\pi^\dagger b_\pi|\Psi_0\rangle$ in the ground state $|\Psi_0\rangle$ is plotted in Fig. 2 as a function of L. Clearly, $\langle\Psi_0|b_\pi^\dagger b_\pi|\Psi_0\rangle$ (as well as the value required for $N_{\rm max}$) grows linearly with the chain length L. In fact, this effect is directly connected to the breaking of the lattice symmetry as can be seen very easily from a very simplified version of Hamiltonian (2). In a symmetry broken state, an effective (approximate) phononic Hamiltonian H_{ph} can be constructed by taking MF values for the spin operators. Assuming that $\sum_i(-1)^i\langle\vec{S}_i.\vec{S}_{i+1}\rangle_{MF}$ (dimer order parameter) varies linearly with L one then gets $H_{ph} = Ag\sqrt{L}(b_\pi+b_\pi^\dagger)+\Omega\, b_\pi^\dagger b_\pi$

(A is an undetermined constant). In this approximation, $\langle b_\pi^\dagger b_\pi \rangle = A^2 g^2 L/\Omega^2$ grows linearly with the length of the chain. In addition, this simple argument also suggests that the occupation number of the π mode scales like the square of the dimensionless coupling g and like the inverse square of the phonon frequency. These intuitive behaviors are indeed well followed as can be seen in Fig. 3 in a large range of parameters.

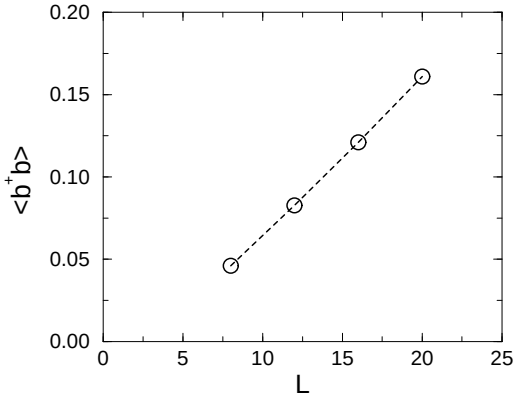

FIG. 2. Dependence of the mean occupation number on the length of the chain L for $g = 0.109$ and $\Omega = 0.3J$.

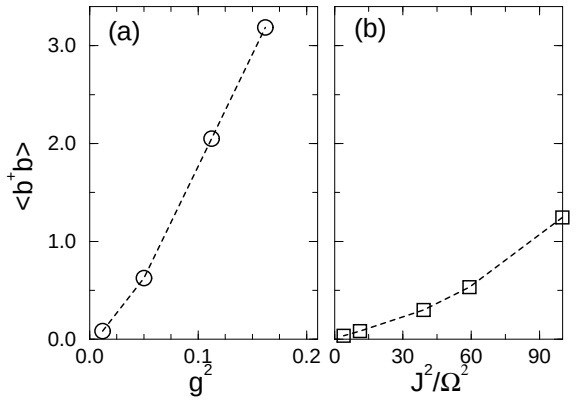

FIG. 3. Mean occupation number calculated on a $L = 12$ site chain versus g^2 for $\Omega/J = 0.3$ (a) and versus $(J/\Omega)^2$ for $g = 0.109$ (b).

One also observes in Fig. 1 that the singlet ground state energy is almost converged for $L = 20$ (the values of the energies for $L = 12$ and $L = 20$ at large $N_{\max}$ are indistinguishable) while finite size effects are still large for the triplet energy because of the existence of a continuum of states above the first triplet excitation. In the next Section, we investigate carefully the convergence of various physical quantities with respect to the system size. We show that an accurate finite size analysis can be performed to obtain extrapolations to the thermodynamic limit.

IV. FINITE SIZE SCALING ANALYSIS

Firstly, we focus on the size dependence of the energy *per site* of the singlet ground state and of the lowest triplet state which are expected to converge to the same value in the thermodynamic limit. Typically, we use chains of length $L = 8$, 12, 16, 20 and 24 sites. Data are shown in Fig. 4 for $\alpha = 0.15$, $g = 0.45$ and $\Omega = 0.3J$. The ground state energy per site varies roughly like $1/L^2$. This behavior is predicted for gapless 1D chains obeying conformal invariance [34] but seems to be still valid here in spite of the presence of a spin gap (see later). This already suggests that, for such parameters, the system sizes are still comparable to the spin correlation length but not much larger. The behavior of the triplet energy is more involved. An approximate $\frac{1}{L}$ dependence is expected (giving a square root singularity in the $1/L^2$ units of Fig. 4) if there is a finite spin gap Δ (defined by the $L \to \infty$ extrapolation of the difference $\Delta(L) = E_0(S = 1, L) - E_0(S = 0, L)$ of the *total* energies of the lowest states of the singlet and triplet spin sectors). Such a behavior seems indeed to be observed in Fig. 4.

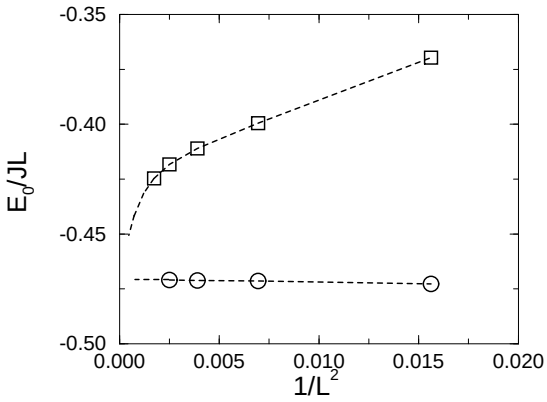

FIG. 4. Convergence of the energy per site of the ground state of spin 0 (∘) and 1 (□) in units of J as a function of the inverse of the square length of the chain $1/L^2$ for $\alpha = 0.15$, $g = 0.45$ and $\Omega = 0.3J$.

Let us now examine in details the behavior of the spin gap $\Delta(L)$ versus L to extract values in the thermodynamic limit. Requiring that the extrapolated ratio Δ/J of the model (2) is equal to the observed experimental value will lead to some constraint on the model parameters Ω and g. Our procedure can be summarised in three steps; (i) a controlled truncation procedure of the phononic Hilbert space for a large set of parameters g, Ω and system sizes L, (ii) a finite size scaling analysis

in order to accurately determine the spin gap as a function of g and Ω; (iii) a determination of the relation to be followed by the parameters g and Ω in order that the calculated ratio Δ/J equals the actual experimental ratio (see Section V).

We first consider the scaling behavior of the spin gap. We have found that it scales accurately according to the law, [35,10]

$$\Delta(L) = \Delta + \frac{A}{L}\exp(-\frac{L}{L_0}), \tag{4}$$

where L_0 is a typical length scale. In general L_0 is of the order of the magnetic correlation length characterizing the decay of the equal time spin-spin correlation in real space. As seen later, values of L_0 are typically 20 lattice units (l.u.) for parameters corresponding to $CuGeO_3$ and 30 l.u. for NaV_2O_5. Therefore, with chains lengths up to 24 sites, finite size effects are still important and an accurate extrapolation is necessary. This scaling is illustrated for $\alpha = 0.15 < \alpha_c$, $g = 0.22$, $\Omega = 0.3J$ ($\circ$), for $\alpha = 0.36 > \alpha_c$ ($CuGeO_3$-like case), $g = 0.089$, $\Omega = 0.3J$ ($\Box$) and for $\alpha = 0$ (NaV_2O_5-like case), $g = 0.40$, $\Omega = 0.5J$ ($\Diamond$) in Fig. 5(a). A spin gap opens for all α if $g > 0$. This is similar to the mean-field treatment where the order parameter $\delta \neq 0$ leads to the symmetry breaking and thus to the opening of a spin gap.

In Fig. 5(b) we compare, in the case of NaV_2O_5 (i.e. $\alpha = 0$), the scaling of the spin gaps calculated using the dynamical model (2) with $g = 0.275$, $\Omega = 0.3J$ ($\circ$) on one hand and the static model (3) with $\delta = 0.05$ ($\Box$) on the other hand [36]. These values of the parameters have been chosen in order to obtain the same extrapolated spin gap. Although the spin gaps are equal, the two models exhibit slightly different scaling behaviors ($L_0 \simeq 30$ for the dynamical model and $L_0 \simeq 18$ for the static one [17]).

At this stage, it is interesting to better understand how in the the dynamical model (2) the opening of the spin gap is connected to the discrete symmetry breaking (as can be seen e.g. in X-rays scattering). The first signature of this phenomenon is the degeneracy of the ground state which is expected in the thermodynamic limit. We have therefore studied the behavior with system size of the energies $E_p(S = 0)$, $p = 0, 1, 2$, of the three lowest singlet states. The energy differences $E_1(S = 0) - E_0(S = 0)$ (circles) and $E_2(S = 0) - E_0(S = 0)$ (squares) are plotted in Fig. 6, in the case $\Omega = 0.3J$, as a function of the inverse length of the chain $1/L$ for $\alpha = 0.36$ (open symbols) and for $\alpha = 0$ (filled symbols). The values of the coupling g are chosen here in such a way to reproduce the experimental spin gaps of the $CuGeO_3$ (open symbols) and NaV_2O_5 (filled symbols) materials (see Section V). The results show very convincingly that the singlet ground state is indeed two-fold degenerate in the thermodynamic limit while a finite gap for singlet excitations appears above [37]. It is important to notice that the quantum numbers associated to the translation symmetry are different for the two lowest singlet states which

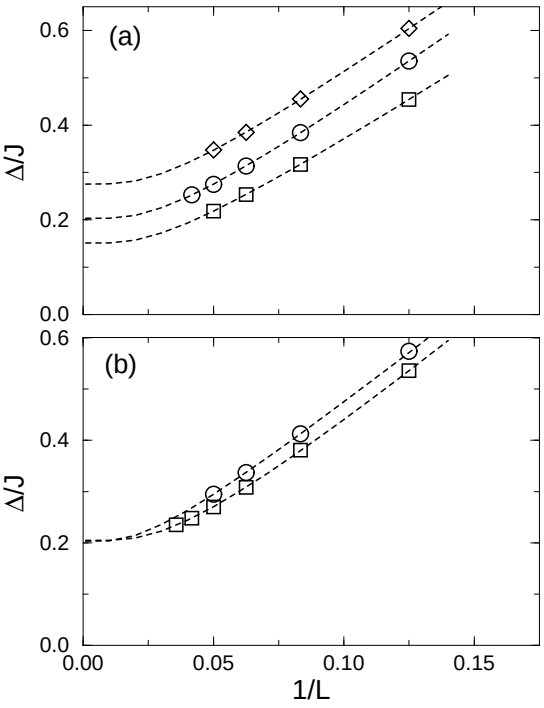

FIG. 5. (a) Spin gap Δ in units of J as a function of the inverse of the length of the chain $1/L$ for $\alpha = 0.15$, $g = 0.22$, $\Omega = 0.3J$ ($\circ$), $\alpha = 0.36$, $g = 0.089$, $\Omega = 0.3J$ ($\Box$) and $\alpha = 0$, $g = 0.40$, $\Omega = 0.5J$ ($\Diamond$). (b) Comparison between the behaviors Δ/J vs $1/L$ obtained within the dynamical model (2) for $\alpha = 0$, $g = 0.275$, and $\Omega = 0.3J$ ($\circ$) and within the static model (3) for $\alpha = 0$, $\delta = 0.05$ ($\Box$).

correspond to momenta $k = 0$ and $k = \pi$. Hence, mixing of these two states leads to a doubling of the unit cell.

The lattice dimerization can be quantitatively measured by the order parameter $\delta^* = \frac{g}{\sqrt{L}}\langle(b_\pi + b_\pi^\dagger)^2\rangle^{1/2}$ (the expectation value $\langle b_\pi + b_\pi^\dagger\rangle$ vanishes because small tunnelling between the two degenerate dimer states always exists in a finite chain). δ^* as a function of the inverse length of the chain is plotted in Fig. 7 for various pairs of parameters (Ω, g) (see caption) chosen in such a way that the spin gap is constant (in fact adjusted to the actual spin gap of $CuGeO_3$ as described in Section V). Extrapolated values of the dimerization δ^* for different phonon frequencies are in fact quite close, at least in the range $0.1 \leq \Omega \leq 0.5$. The dimerization δ^* seems then to be only determined by the magnitude of the spin gap. The fact that δ^*, at fixed extrapolated spin gap, is independent of the frequency Ω is consistent with the proof by Brandt and Leschke [21] that the thermodynamic properties of the dynamical model (2) and of the static model (3) are identical. However, it is interesting to notice that the value obtained here (~ 0.022) is significantly larger than the value (~ 0.014) needed in the MF approximation to produce the same gap. The differ-

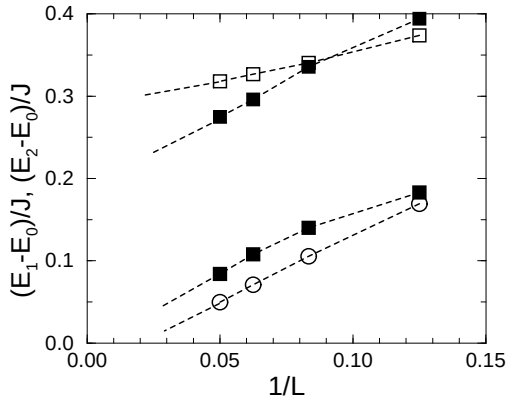

FIG. 6. Energy differences $(E_1(S=0)-E_0(S=0))/J$ $(\circ,\bullet)$ and $(E_2(S=0)-E_0(S=0))/J$ $(\square,\blacksquare)$ as a function of $1/L$. Open and filled symbols correspond to $\alpha=0.36$, $g=0.109$ and $\Omega=0.3J$ and to $\alpha=0$, $g=0.270$ and $\Omega=0.3J$, respectively.

ence between these two values can be simply attributed to the zero point motion of the harmonic mode which is included only in (2).

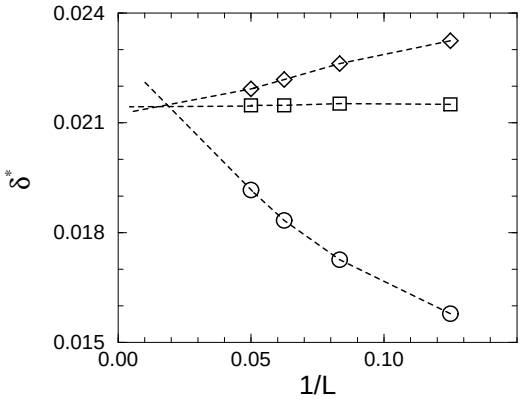

FIG. 7. Order parameter δ^* as a function of the inverse of the length of the chain $1/L$ for $\Omega=0.1J$ and $g=0.062$ $(\circ)$, $\Omega=0.3J$ and $g=0.109$ $(\square)$ and $\Omega=0.5J$ and $g=0.141$ $(\diamond)$ (see text regarding the choice of parameters).

V. COMPARISON WITH EXPERIMENT

The systematic finite size scaling described above has been performed for a large set of parameters Ω/J and g. For simplicity, let us first assume $\Omega/J=0.3$. The behavior of $\Delta(\Omega/J=0.3,g)/J$ versus g is plotted in Fig. 8 for a large frustration $\alpha=0.36$ corresponding to the case of $CuGeO_3$ $(\circ)$ and for a non frustrated chain corresponding to the case of NaV_2O_5 $(\square)$. Quite generally, the spin gap grows with the coupling constant g as expected. Indeed, a larger coupling to the lattice produces a larger dimerization and then, indirectly, a larger spin gap.

The actual physical value of the ratio Ω/J is, to the best of our knowledge, difficult to obtain from experiment. Therefore, we shall not here restrict to any specific value of Ω/J but rather consider a wide range $0.1\leq\Omega/J\leq 0.5$. However, for each value of Ω, the dimensionless coupling constant $g(\Omega)$ can be determined by enforcing that the extrapolated spin gap ratio $\Delta(\Omega,g)/J$ equals the experimentally observed gap. The procedure is shown in Fig. 8 for $\Omega=0.3J$ and $\alpha=0$ (NaV_2O_5) and $\alpha=0.36$ ($CuGeO_3$). The small horizontal marks correspond to the actual experimental gaps, i.e. $\Delta/J\simeq 0.151$ and $\Delta/J\simeq 0.193$ for $CuGeO_3$ and NaV_2O_5, respectively. We then obtain $g(\Omega=0.3)\simeq 0.109$ for $CuGeO_3$ and $g(\Omega=0.3)=0.270$ for NaV_2O_5. The same method was performed for two other values of the frequency, $\Omega=0.1J$ and $\Omega=0.5J$. A relation is then obtained between Ω and g for the two values of the frustration parameter $\alpha=0$ and $\alpha=0.36$. This is illustrated in Fig. 9. We find that Ω has to vary roughly like g^2 in order that the spin gap is constant. Naively, one indeed expects that softer (*i.e.* with smaller Ω) phonon modes are more effective to break the lattice symmetry. So, if one requires the spin gap to be constant, this effect has to be compensated by a smaller coupling g.

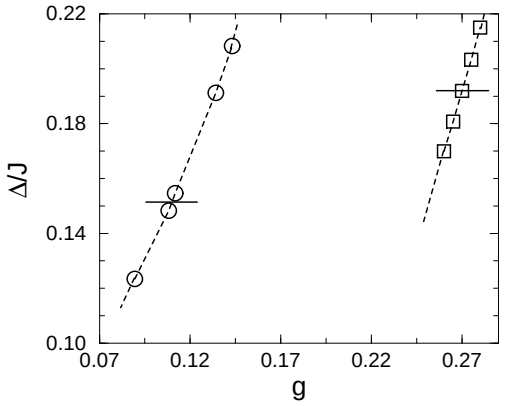

FIG. 8. Spin gap Δ/J (in units of J) as a function of the magneto-elastic coupling g for $\alpha=0.36$, $\Omega=0.3J$ $(\circ)$ and $\alpha=0$, $\Omega=0.3J$ $(\square)$. Horizontal marks indicate actual experimental spin gap values.

In Fig. 9 we observe that the coupling constant $g(\Omega)$ is roughly $2.5-3$ times smaller for $CuGeO_3$ than for NaV_2O_5 although the ratio of their spin gaps is only 1.5. This is an interesting consequence of the large frustration in $CuGeO_3$. Indeed, a large α opens alone a (quite small) spin gap and, more importantly, amplifies the effect of the

spin-phonon coupling. This effect is even more drastic in the static model (3) where the dimerizations $\delta = 0.014$ ($CuGeO_3$) and $\delta = 0.048$ (NaV_2O_5) have a ratio of about 4 [17].

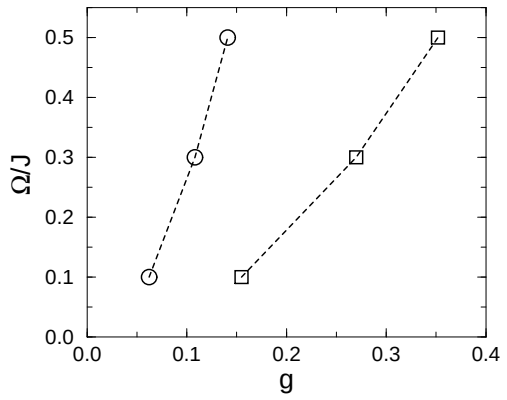

FIG. 9. Frequency Ω in units of J as a function of the magneto-elastic coupling g insuring a constant spin gap (see text) for $\alpha = 0.36$ ($\circ$) and $\alpha = 0$ ($\Box$).

The model (2) seems to describe accurately the spin-Peierls transition. Theoretical parameters have been deduced from experiment and the ground state properties of the spin-Peierls phase have been established. We have provided evidences in favour of the dynamical breaking of the lattice periodicity with the simultaneous opening of the spin gap. Next, we shall study the dynamical properties of this model.

VI. DYNAMICAL PROPERTIES

INS is a powerful experiment probing the momentum-dependence of the spin dynamics. INS has been performed on $CuGeO_3$ single crystals [13,12] and on NaV_2O_5 powders [3]. It provides a direct measure of the dynamical spin-spin structure factor,

$$S_{zz}(q,\omega) = \sum_n |\langle \Psi_n | S_z(q) | \Psi_0 \rangle|^2 \delta(\omega - E_n + E_0), \quad (5)$$

where $|\Psi_0\rangle$ is the (singlet) ground state of energy E_0 and the sum is performed on all triplet excited states $|\Psi_n\rangle$ (of energy E_n). $S_z(q)$ is normalised as $1/\sqrt{L}\sum_j \exp(iqj) S_j^Z$.

The INS spectrum can be easily computed by exact diagonalization techniques [33]. Results on a 20 site chain are shown in Fig. 10(a) for $CuGeO_3$ and in Fig. 10(b) for NaV_2O_5 with a frequency $\Omega = 0.3J$. In both cases we observe a well defined q-dependent low energy structure as for the static model (3). Its bandwidth (i.e. the energy at the maximum of the dispersion at $q = \pi/2$) is typically $\omega_{max} \sim 1.1J$ for $CuGeO_3$ and $\omega_{max} \sim 1.6J$ for NaV_2O_5. This second value is very close to the DesCloizeaux-Pearson value of $\pi/2$ [38] of the Heisenberg chain in contrast to the case of $CuGeO_3$ which exhibits a large frustration. The ratio ω_{max}/J could therefore be considered as an additional accurate measure of the amount of frustration within the chain since the parameter α alone determine approximately ω_{max}/J. It is interesting to notice also that, in the case of a frustrated chain ($CuGeO_3$), the upper limit of the continuum seems to be better defined.

At low energy, the dimerization gap leads to major differences with respect to the Heisenberg chain. First, there is no intensity for $\omega < \Delta$. Secondly, the magnon branch is well separated from the continuum by a finite gap (see below) so that the magnon excitation can be interpreted as a spinon-spinon bound state [23]. This bound state was also found in the static model (3) for $CuGeO_3$ [24,19] and NaV_2O_5 [17].

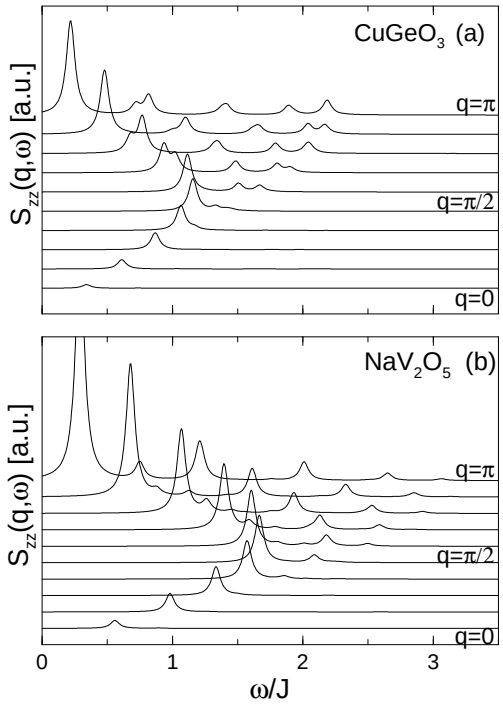

FIG. 10. $S_{zz}(q,\omega)$ as a function of ω/J calculated on a 20 site chain for $q = n\frac{\pi}{10}$, $n = 0, \cdots, 10$; (a) $CuGeO_3$ parameters, $\alpha = 0.36$, $g = 0.109$, $\Omega = 0.3J$; (b) NaV_2O_5 parameters, $\alpha = 0$, $g = 0.270$, $\Omega = 0.3J$. A broadening of the δ-functions $\varepsilon = 0.04J$ was used.

The dispersion relations of the magnon branch ($\circ$), the second excitation ($\Box$) and the upper limit of the continuum ($\diamondsuit$) in the dynamical model (2) are plotted in Fig. 11(a) for $CuGeO_3$. The '$*$' symbols correspond to experimental results from Ref. [13] and filled symbols correspond to infinite size extrapolations at momenta $q = \pi/2$ and $q = \pi$. Similar dispersion relations are shown in

Fig. 11(b) for NaV_2O_5 and the position of the experimental $q = \pi$ spin gap [3] is indicated by an arrow. Note that we have explicitly checked that the magnon branch is well separated from the continuum. A finite size scaling analysis of the energies of the two lowest triplet states (•,■) is indeed possible at momentum $q = \pi/2$. Figs. 11(a-b) clearly show that there is a finite gap between the first branch and the continuum as in the static model. It is consistent with the fact that the continuum corresponds to solitonic spin-1/2 excitations (or spinons) and that solitons and antisolitons can bind in pairs with momenta close to $q = \pi/2$ [23]. Such a dougle gap feature was indeed observed experimentally [39].

It is important to notice that the dispersion relation is not symmetric with respect to $q = \pi/2$ in contrast to the case of a static dimerization. In fact, such a symmetry in the energy spectrum is due to the Bragg scattering resulting from the doubling of the unit cell. Since the dimerization appears only as a true phase transition in model (2), we expect that the symmetry of the spectrum with respect to $\pi/2$ will only become exact in the thermodynamic limit. In the case of $CuGeO_3$, our results are in very good agreement with INS experiments although finite size effects are still important. In fact the agreement improves with increasing system size since the calculated magnon branch for $q > \pi/2$ shifts slightly to lower energy when L grows (in order to be symmetric with the $q < \pi/2$ part). Note also that energy scales are four times larger for NaV_2O_5 than for $CuGeO_3$ which could restrict INS experiments on NaV_2O_5 to low energy regions of the spectrum in the vicinity of $q = \pi$.

It is interesting to compare results for the spin dynamics obtained within the dynamical model to the ones obtained within the static model. Fig. 12 shows the lowest triplet magnon branches and the next triplet excitations (in fact lower limits of the $S = 1$ continuum) for parameters suitable for $CuGeO_3$. We do not explicitly show the comparison of the upper limits of the continua since the two curves obtained within the two models are almost indistinguishable. This is not surprising because higher energy excitations are only determined by the magnitude of the frustration and the coupling to the lattice plays a minor role here. At lower energy, the magnon branches of the two models look also very similar for $q < \pi/2$ but some differences appear for $q > \pi/2$ since, as explained before, the dispersion is not symmetric with respect to $\pi/2$ in the dynamical model. This is simply due to larger finite size effects [40] occurring in model (2) related to the fact that the lattice periodicity is only *spontaneously* broken. Once such finite size effects are taken into account we can safely conclude that the dispersions of the magnon branches of the two models in the thermodynamic limit are very close. Similarly, the discrepancies seen between the positions of the lower limits of the continua of triplet excitations are not relevant. Indeed, a detailed finite size scaling analysis at e.g. $q = \pi/2$ reveals that the position of the two lower limits are in fact quite close ($1.117J$ for (3) to be compared to $1.118J$ for (2)). An exactly similar

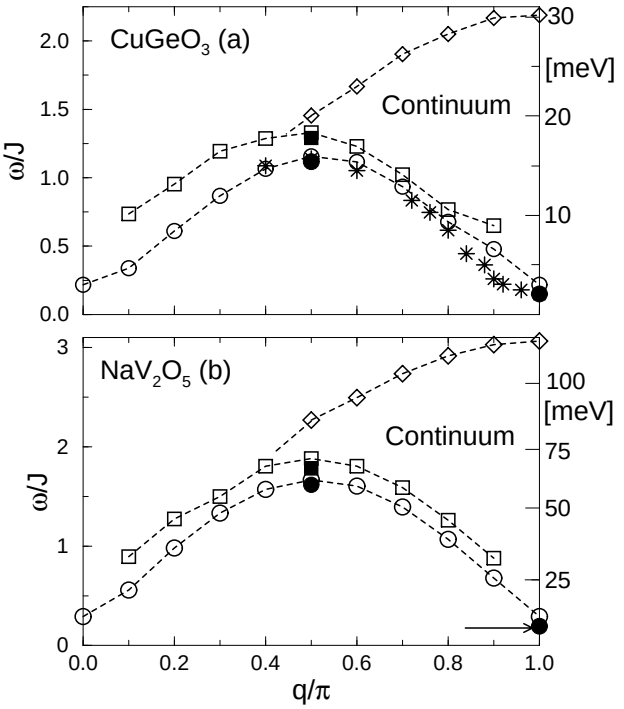

FIG. 11. Momentum dependence of the first (○), second excitation (□) and upper limit of the continuum (◊) on a 20 site chain for the dynamical model (2). Filled symbols represent extrapolations to infinite size (first (•) and second (■) excitations). (a) $CuGeO_3$ parameters ($\alpha = 0.36$, $g = 0.109$, $\Omega = 0.3J$). Experimental values (∗) are taken from from Ref. [13]. Units on the right are in meV assuming $J = 160K$ (13.8 meV). (b) NaV_2O_5 parameters ($\alpha = 0$, $g = 0.270$, $\Omega = 0.3J$). Units on the right are in meV assuming $J = 440K$ (37.9 meV). The arrow indicates the experimental value of the $q = \pi$ spin gap.

comparison can be done for NaV_2O_5 (not shown).

The spin static structure factor,

$$S_{zz}(q) = \int d\omega S_{zz}(q,\omega) \ ,$$

which can be obtained in INS by integrating the spectrum over energy is plotted in Fig. 13 for $CuGeO_3$ ($\alpha = 0.36$, $g = 0.109$, $\Omega = 0.3J$) (○) and NaV_2O_5 (•) ($\alpha = 0$, $g = 0.270$, $\Omega = 0.3J$) for a 20 site chain. It is peaked near $q = \pi$ as a result of strong short range AF correlations. Indeed the width of the peak at $q = \pi$ is directly related to the inverse magnetic correlation length. Note however that $S_{zz}(\pi)$ is slightly suppressed in $CuGeO_3$ compared to NaV_2O_5 because of the interchain frustration. In any case, the results are very similar to those obtained with the static dimerized model. The relative weights of the magnon peak in $S_{zz}(q,\omega)$ are also shown for $CuGeO_3$ (□) and NaV_2O_5 (■). Their behaviors versus q suggest that working in a range of momenta around $q = 0.8\pi$ might be

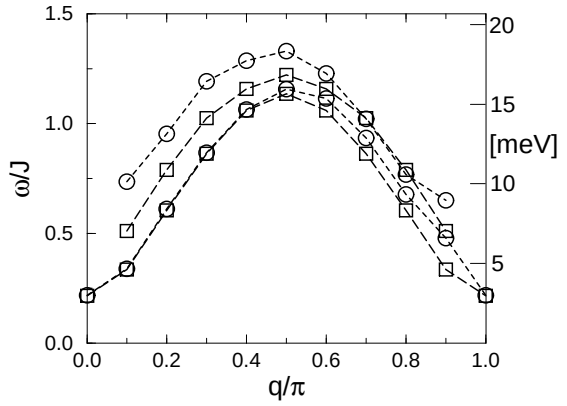

FIG. 12. Momentum dependence of the two lowest triplet excitation energies in $CuGeO_3$ calculated on a 20 site chain for (i) the dynamical model (2) ($\alpha = 0.36$, $g = 0.109$, $\Omega = 0.3J$) ($\circ$) and (ii) the static model (3) ($\alpha = 0.36$, $\delta = 0.014$) ($\square$). Units on the right are meV assuming that $J = 160K$ (13.8 meV).

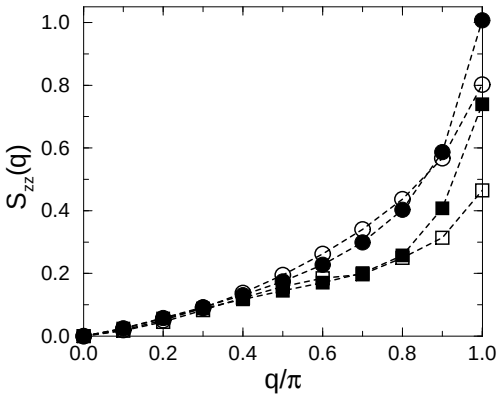

FIG. 13. Static factor structure for $CuGeO_3$ ($\alpha = 0.36$, $g = 0.109$, $\Omega = 0.3J$) ($\circ$) and NaV_2O_5 ($\alpha = 0$, $g = 0.270$, $\Omega = 0.3J$) ($\bullet$) calculated on a 20 site chain. Squares correspond to the weight of the lowest peak for $CuGeO_3$ ($\square$) and for NaV_2O_5 ($\blacksquare$).

more appropriate experimentally in order to have clearer evidences for the continuum.

VII. CONCLUSIONS

In order to describe one dimensional spin-Peierls compounds, a magneto-elastic (i.e. spin-phonon) coupling has been considered and is shown to be responsible for a dynamical and spontaneous breaking of the lattice periodicity followed simultaneously by the opening of a spin gap. The resulting symmetry-broken ground state is consistent with the existence of a frozen dimerization such as the one obtained in a mean-field treatment of the coupling to the lattice. We have used exact diagonalization techniques to calculate static and dynamical properties of this model. Controlled truncation procedures have been applied to the bosonic Hilbert space of the Hamiltonian. By using a finite size scaling analysis, we have compared various physical quantities to the experimental ones (in the case of $CuGeO_3$ and NaV_2O_5) and we have determined a range of suitable parameters for the model. We predict that the spin-phonon coupling is 2 or 3 times larger in NaV_2O_5 than in $CuGeO_3$. The INS spectrum calculated within this model is found to be qualitatively similar to the one obtained in the static model with a finite gap separating the magnon branch from the continuum of triplet excitations above.

D.A. acknowledges useful discussions with M. Albrecht and S. Capponi. We thank L. P. Regnault for communicating to us the data of Ref. [13], J. Riera for valuable comments and IDRIS (Orsay) for allocation of CPU time on the C94 and C98 CRAY supercomputers.

After completion of this work, we learnt of a related work by A. W. Sandvik *et al.* (cond-mat/9706046) using a Quantum Monte Carlo approach.

[1] M. Hase, I. Terasaki, and K. Uchinokura, Phys. Rev. Lett. **70**, 3651 (1993).
[2] M. Isobe and Y. Ueda, J. Phys. Soc. Jpn. **65**, 1178 (1996).
[3] Y. Fujii et al., J. Phys. Soc. Jpn. **66**, 326 (1997).
[4] T. Ohama, M. Isobe, H. Yasuoka and Y. Ueda, J. Phys. Soc. Jpn. **66**, 545 (1997).
[5] M. Weiden, R. Hauptmann, C. Geibel, F. Steglich, M. Fischer, P. Lemmens and G. Güntherodt, preprint cond-mat/9703052.
[6] J. P. Pouget *et al.*, Phys. Rev. Lett. **72**, 4037 (1994); Q.J. Harris *et al.*, Phys. Rev. B **50**, 12 606 (1994).
[7] J. Riera and A. Dobry, Phys. Rev. B **51**, 16098 (1995).
[8] G. Castilla, S. Chakravarty, and V. J. Emery, Phys. Rev. Lett. **75**, 1823 (1995)
[9] J. Riera and S. Koval, Phys. Rev. B **53**, 770 (1996).
[10] G. Bouzerar, A. P. Kampf and F. Schönfeld, preprint cond-mat/9701176.
[11] F. Mila, P. Millet and J. Bonvoisin, Phys. Rev. B **54**, 11 925 (1996).
[12] M. Nishi, O. Fujita and J. Akimitsu, Phys. Rev. B **50**, 6508 (1994).
[13] L. P. Regnault, M. Aïn, B. Hennion, G. Dhalenne and A. Revcolevschi, Phys. Rev. B **53**, 5579 (1996).
[14] M. Itoh, M. Sugahara, T. Yamauchi and Y. Ueda, Phys.

Rev. B **53**, 11 606 (1996).
[15] F. D. M. Haldane, Phys. Rev. B **25**, 4925 (1982).
[16] K. Okamoto and K. Nomura, Phys. Lett. A **169**, 433 (1992).
[17] D. Augier, D. Poilblanc, S. Haas, A. Delia and E. Dagotto, Phys. Rev. B **56**, Rxxx (1997).
[18] S. Haas and E. Dagotto, Phys. Rev. B **52**, R14396 (1995).
[19] D. Poilblanc, J. Riera, C. A. Hayward, C. Berthier and M. Hortavić, Phys. Rev. B **55**, Rxxx (May, 1997).
[20] V. N. Muthukumar *et al.*, Phys. Rev. B **54**, R9635 (1996).
[21] U. Brandt and H. Leschke, Z. Physik **271**, 295 (1974); see also K. Hepp and E.H. Lieb, Phys. Rev. A**8**, 2517 (1973).
[22] Multiple phonons have been considered in related models of correlated electrons by e.g. R. Fehrenbacher, Phys. Rev. B **49**, 12 230 (1994) and G. Wellein, H. Röder and H. Fehske, Phys. Rev. B **53**, 9666 (1996) in one and two dimensions respectively.
[23] G. S. Uhrig and H. J. Schulz, Phys. Rev. B **54**, R9624 (1996); for a discussion on soliton confinement see e.g. I. Affleck, preprint cond-mat/9705127.
[24] A. Fledderjohann and C. Gros, Europhys. Lett. **37**, 189 (1997).
[25] A detailed review on electron-phonon interaction in one-dimensional correlated electron systems can be found in "One-dimensional Fermi liquids", J. Voit, Rep. Prog. Phys. **58**, 977 (1995).
[26] W. Stephan, M. Capone, M. Grilli and C. Castellani, preprint cond-mat/9605164; D. Khomskii, W. Geerstma and M. Mostovoy, Czech. Journ. of Phys. **46**, Suppl. S6, 32 (1996).
[27] T. Tonegawa and I. Harada, J. Soc. Jpn. **56**, 2153 (1987).
[28] R. Chitra, S. Pati, H. R. Krishnamurthy, D. Sen and S. Ramasesha, Phys. Rev. B **52**, 6581 (1995).
[29] In two dimensional systems, similar approaches can be found e.g. in A. Dobry, A. Greco, S. Koval and J. Riera, Phys. Rev. B **52**, 13 722 (1995); D. Poilblanc, T. Sakai, W. Hanke and D. J. Scalapino, Europhys. Lett. **34**, 367 (1996).
[30] S. Capponi, N. Guihéry, J.-P. Malrieu, B. Miguel and D. Poilblanc, Chemical Physics Letters **255**, 238 (1996); for models with no electronic correlations see W. P. Su, J. R. Schrieffer and A. J. Heeger, Phys. Rev. Letters **42**, 1698 (1979).
[31] The equivalence has been rigorously established by Ref. [21] for the Fröhlich Hamiltonian and should be also exact for model (2) which includes correlations between electrons.
[32] To the best of our knowledge, no proof exists that *dynamical* correlations should be identical.
[33] For a review on numerical methods based on the Lanczos algorithm, see e.g. "Exact diagonalisation methods for models of strongly correlated fermions", D. Poilblanc in *Numerical methods for strongly correlated systems*, Ed. D. J. Scalapino, Frontiers in physics (1997).
[34] H. Frahm and V. E. Korepin, Phys. Rev. B **42**, 10 553 (1990).
[35] M. N. Barber, in *Phase transitions and critical phenomena*, Vol. 8, Ed. C. Domb and J. L. Lebowitz (Academic, London, 1983).
[36] For the static model (3), chains with up to $L = 28$ sites were considered.
[37] The second singlet double-magnon excitation energy is roughly twice larger than the first triplet excitation (for more details see e.g. [17]). However, singlet phononic excitations may lie below the continuum.
[38] J. Des Cloiseaux and J. J. Pearson, Phys. Rev. **128**, 2131 (1962).
[39] M. Aïn, J. E. Lorenzo, L. P. Regnault, G. Dhalenne, A. Revcolevschi, B. Hennion and Th. Jolicoeur, Phys. Rev. Lett., **78**, 1560 (1997).
[40] As can be seen e.g. in the finite size extrapolations of the triplet excitations energies at $q = \pi/2$. In contrast, in the static model (3), the computed data [19,17] are almost indistinguishable from the extrapolated values.